ISSN 8755-6839

SCIENCE OF TSUNAMI HAZARDS

Journal of Tsunami Society International

Volume 31 Number 3 2012

CATASTROPHIC FLANK COLLAPSE ON TA'U ISLAND AND SUBSEQUENT TSUNAMI: HAS THIS OCCURRED DURING THE LAST 170 YEARS?

Shaun Williams, Tim Davies, Jim Cole

Natural Hazards Research Centre
Department of Geological Sciences
University of Canterbury, PB 4800
Christchurch, New Zealand

ABSTRACT

Ta'u, the easternmost inhabited island in the Samoan Islands archipelago, exhibits a series of down-faulted benches on its southern flank, believed to be the remnant of ~30 km^3 catastrophic collapse. A historical map of Ta'u charted in 1839 during the United States Exploring Expedition, which did not show the benches, suggests that the event occurred less than 170 years ago. A collapse event of this magnitude would have generated a locally devastating tsunami, with possible impacts experienced at the regional level. However, no written or oral records of such an event exist. A number of key questions thus emerge, and formed the basis for this study. Did this event actually happen within the last 170 years, and if so, how and why could it have gone unnoticed? Or, is the event much older than the impression obtained from the literature? The catastrophic flank collapse was modeled using 100 m contour-resolution bathymetry data of the Ta'u region, coupled with rational assumptions made on the geometry of the failed mass. This enabled numerical landslide-tsunami simulation in the Cornell Multigrid Coupled Tsunami Model (COMCOT). The results indicate that if an event of this magnitude occurred in the last 170 years, it could not have gone unnoticed by local inhabitants. It thus seems likely that the initial survey conducted during the Exploring Expedition was inaccurate. Nevertheless, the well-preserved nature of the benches indicates collapse relatively recently and raises the possibility of future collapse.

Keywords: *Volcanic flank collapse, Ta'u Island volcano, tsunami,*

1. INTRODUCTION

Ta'u is the easternmost inhabited island in the Samoa Islands volcanic chain (Figure 1). It lies within the Manu'a Group of the Territory of American Samoa, and has three populated villages: Faleasao and Ta'u villages in the northwest, and Fitiuta village in the northeast. The total population of the island is just under 1000 (U.S. Census Bureau, 2000). The island has a total land area of ~46 km^2, with a summit ~925 m above mean sea level. It is located ~104 km east of Tutuila, the capital island of American Samoa.

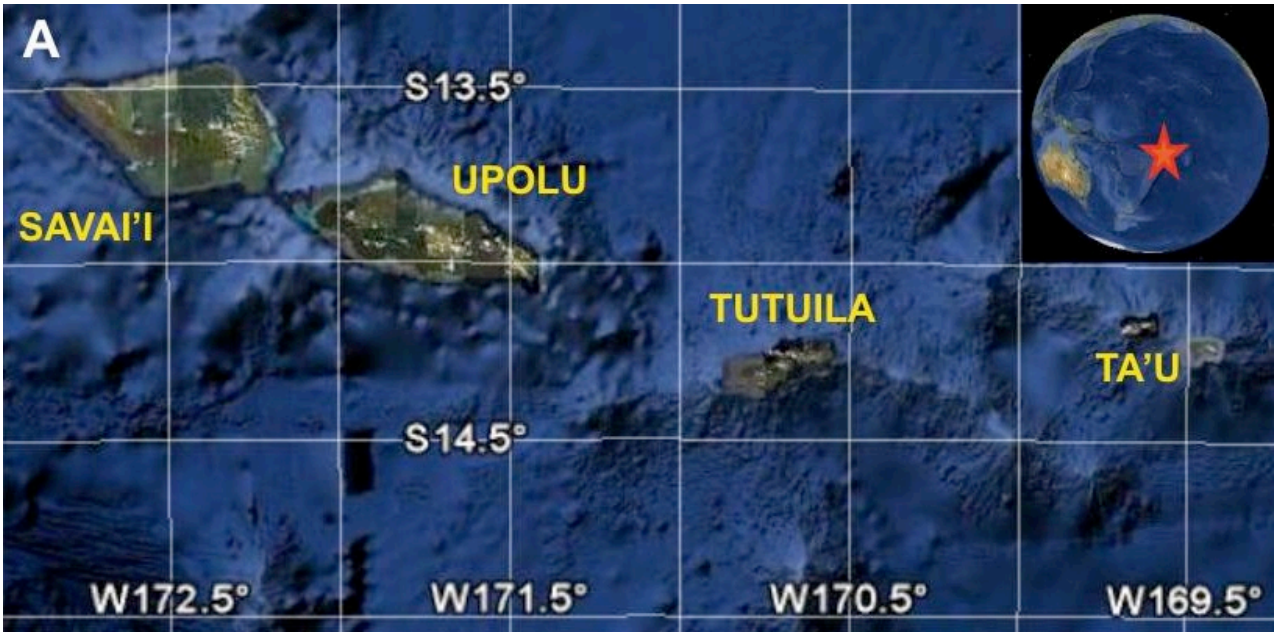

Figure 1: Location map of the Samoan Islands (Map source: Google Earth).

Geologically the island is in a shield-building stage of volcanism (Macdonald and Abbott, 1970; Natland, 1980; Natland and Turner, 1985), although the nature of recent historical eruptions is uncertain. The island (and surrounding islands) have been inhabited for more than 3000 years (Nunn, 1994, 1998), but oral traditions only extend back a little under 1000 years (Linnekin et al, 1995), leaving no oral tradition regarding the ages of events before this time.

On the south flank of the island is apparently the remnant of a large-scale flank collapse with a total estimated volume of about 30 km^3 (Figures 2 and 3). Similar large-scale collapse features and resulting debris-avalanche deposits have also been recognized on the submarine slopes of Savai'i and Upolu (Hill and Tiffin, 1993; Keating and McGuire, 2000; Keating et al., 2000). The first internationally published map of the Samoa Islands was presented in Turner (1889), which depicts Ta'u as having a rounded, regular, dome-shaped morphology, with twice the present-day land area (Figure 4). All of the other islands along the chain look similar (morphologically) in the map as they do today; Ta'u is an obvious anomaly in this respect.

Figure 2: Photograph of the south flank of Ta'u (Photo by: Michael Tennant, Dec-2006).

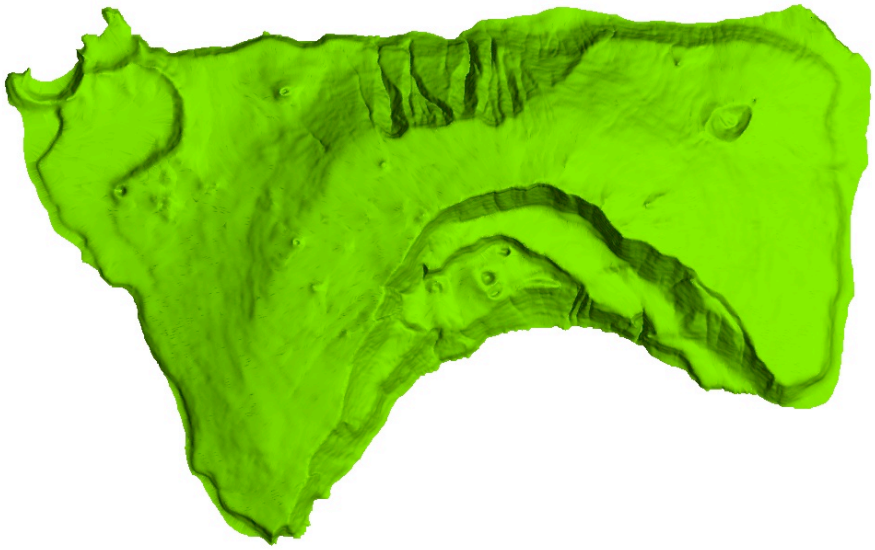

Figure 3: Digital elevation model of Ta'u Island showing the series of down-faulted benches on its southern flank.

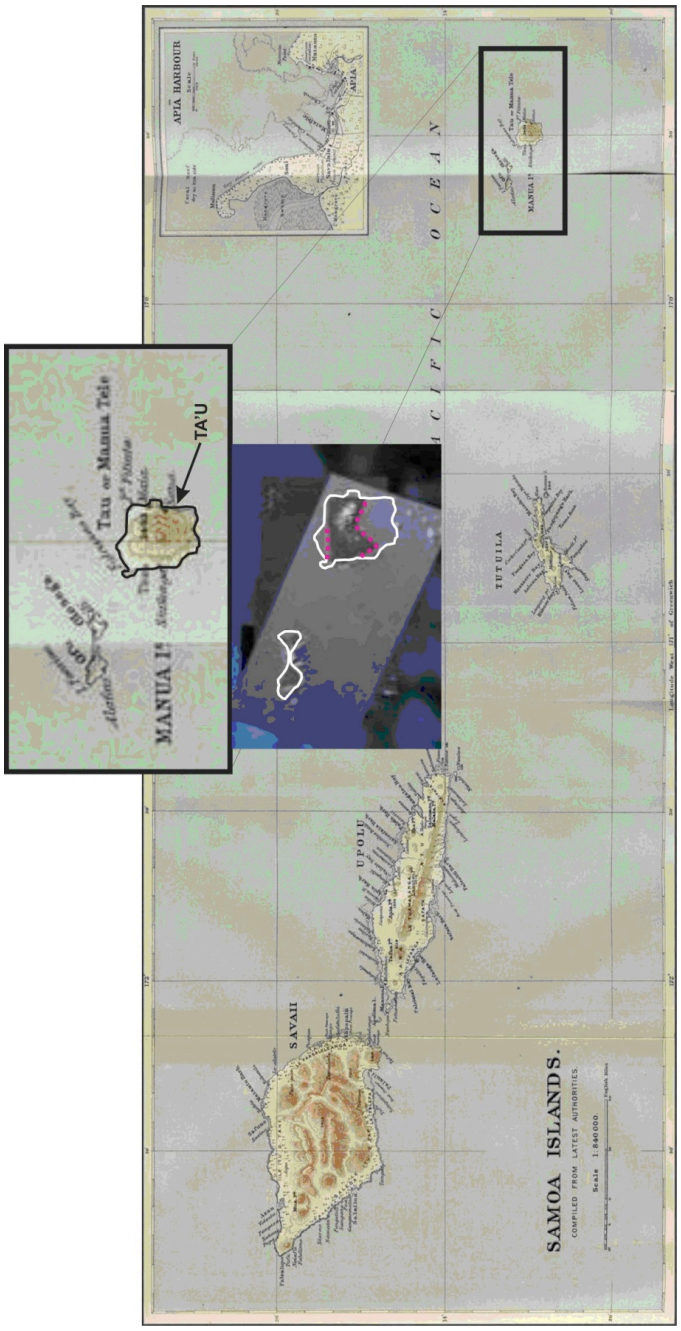

Figure 4: Historical map of the Samoa Islands presented in Turner (1889). A blow-up of the Manu'a group is given, and a simple map overlay to illustrate the obvious anomaly in the morphological depiction of Ta'u from its present shape. Ofu and Olosega Islands in the map-overlay illustrate an example of how other islands in the chain more or less looked the same then as they do today.

The map in Turner (1889) was based on the original survey charts of Charles Wilkes, who commanded the 1838 – 1842 U.S Exploring Expedition; the first United States government funded circum-navigational scientific exploring expedition. Wilkes reported that three days were spent accurately surveying the coasts of the Manu'a group. Ta'u was described as having the form of a regular dome (Figure 5), with an estimated land area of ~259 km^2. This strengthens the likelihood that large-scale collapse may have been recent. Given the oceanic environment in which collapse occurred, a large-scale local tsunami would have been generated with definite local catastrophic, and possibly regional, impacts. Interestingly, no written or oral documentation regarding such an event exists.

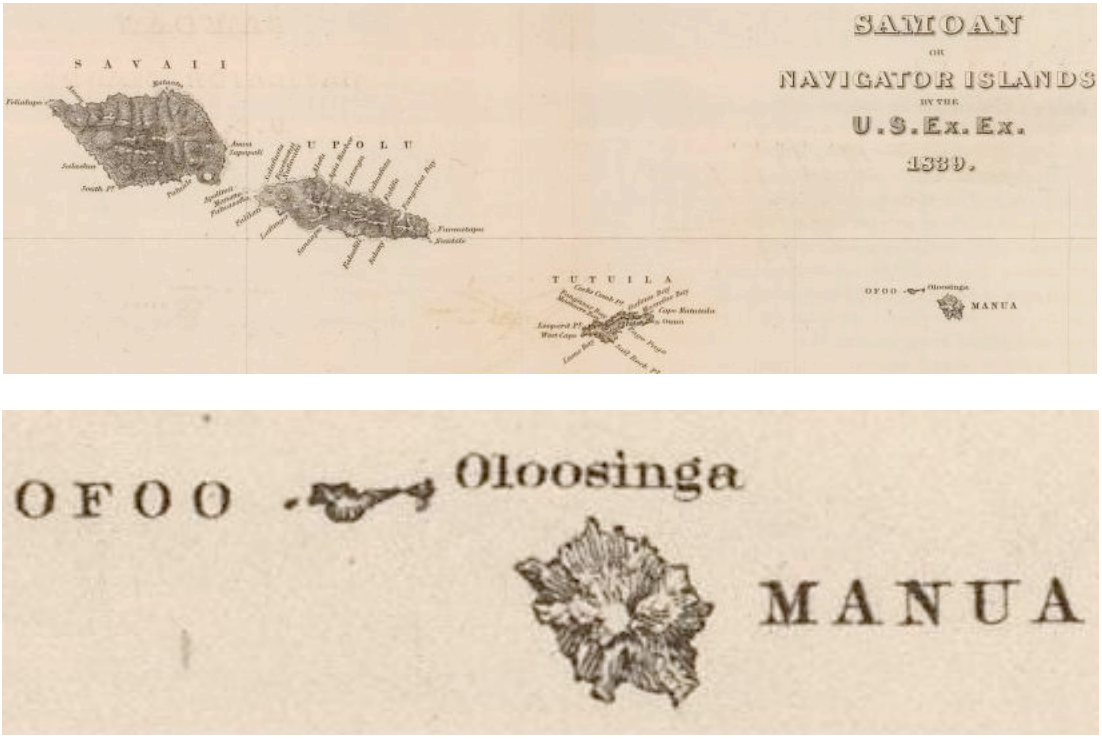

Figure 5: Map of the Samoa Islands charted in 1839 during the U.S.N. Charles Wilkes Expedition (from Wilkes, 1849). The bottom image is a blow-up of the eastern Manu'a Group from the top map; and depicts a rounded Ta'u morphology

Hence a number of questions emerge. On the one hand, there appears to be an obvious dilemma associated with the information described by Wilkes (1849), and later presented by Turner (1889). Were these early observations and resulting map indeed an accurate depiction of Ta'u in the mid to late 19th century? If so, why is there no written or oral account of the collapse? Is it possible that such an event went unnoticed? Or, could the map represent a significant cartographic error? If it does, it would raise serious debate regarding the reliability of the reported observations of Ta'u during the Charles Wilkes Expedition.

A review of the physical characteristics of Ta'u is presented here, including aspects of the island's geology and geomorphology with specific emphasis on evidence relevant to the nature and timing of the collapse, is followed by a tsunami modelling assessment. This involves numerical simulation of the flank-collapse using available data; the results have significant indirect implications for the timing of the event.

2. METHODS

A literature review combining geology and geomorphology was used to establish a solid information platform for understanding the relative timing and nature of physical processes in the area. Geomorphic analysis based on 10 m contour resolution topography data, 100 m contour resolution bathymetry data, and empirical observations were used to obtain a better understanding of significant morpho-structures in the area (Figure 6). It also enhanced understanding of the timing of formation of the collapse feature. Field observations in February and August 2008 were also undertaken to verify some of these features.

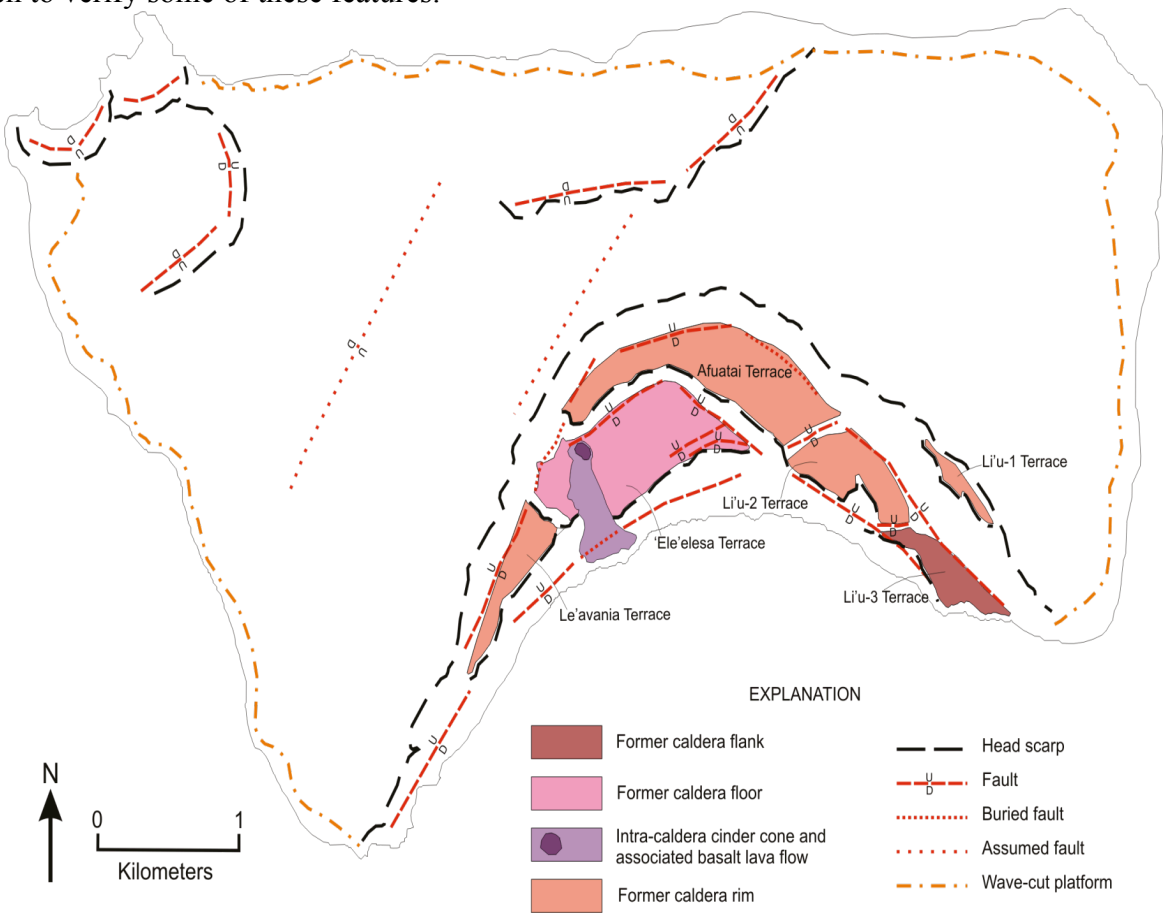

Figure 6: Main geomorphic features on the south flank of Ta'u; inferred using 10 m contour resolution data.

100 m contour resolution bathymetry data coupled with 3D analysis in the Vulcan 7.5 software was used to identify offshore features possibly associated with a collapse deposit, enabling rational assumptions to be made on the geometry of past collapse.

The Cornell Multi-grid Coupled Tsunami (COMCOT) model (version 1.7: Wang, 2009)) was used to model a range of landslide-induced tsunami scenarios; the landslides are hereafter referred to as submarine mass failures (SMF). COMCOT consists of a built-in set of complex algorithms that calculate and output ocean volume flux within a simulated grid, using bathymetry data as well as geometric characterizations of a failing mass. For this study, linear shallow water equations were used to describe water surface elevation and ocean flux in both spherical and Cartesian coordinate systems. An explicit leapfrog finite difference method was used to solve these equations in time and space for each grid cell within the simulation domain (Figure 7).

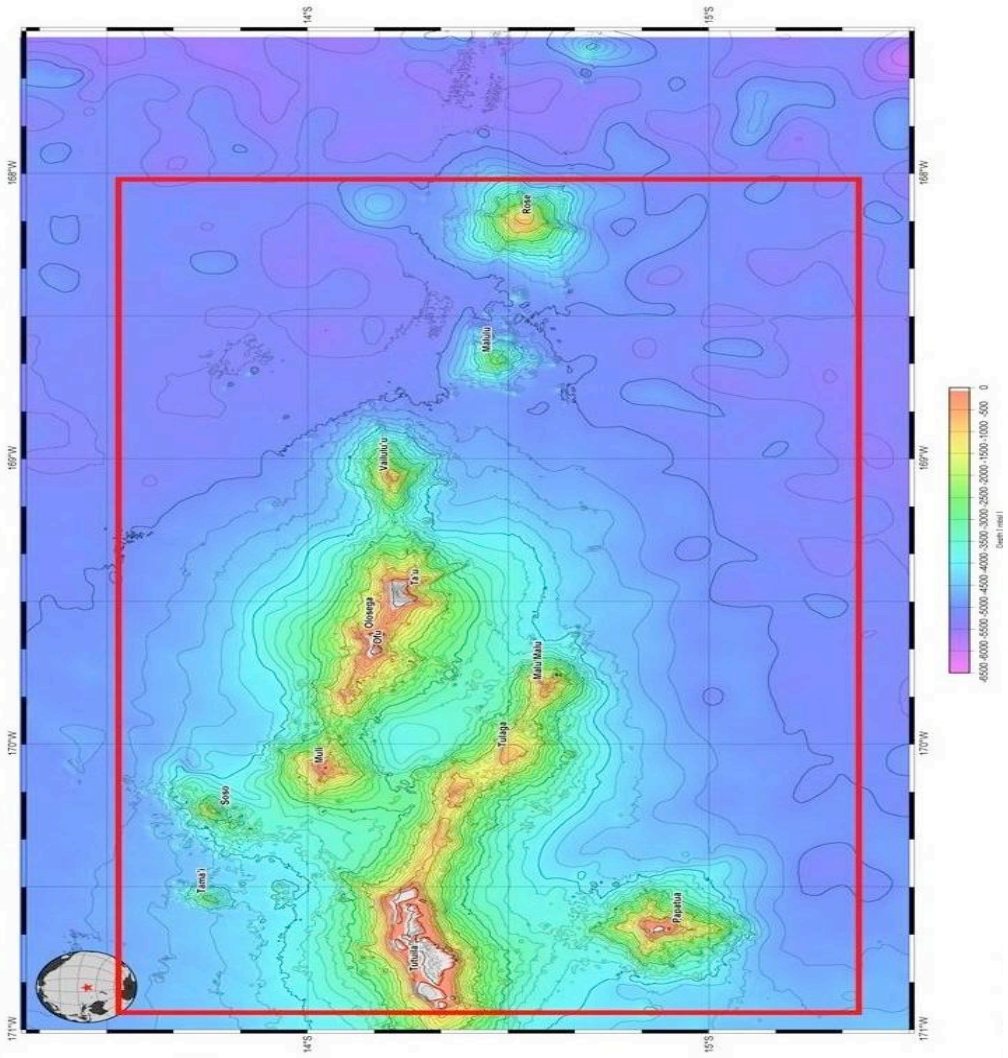

Figure 7: Merged bathymetry map of American Samoa; Region 14.3 S, 170.0 W (Source: http://earthref.org). Contour interval = 200 m. The red border indicates the numerical (simulation) domain.

Output data were visualized through post-processing using Matlab functions and scripts developed by Wang (2009). 100 m contour resolution multi-beam bathymetry data collected during the Alia Scientific Cruise Expedition in April 2005 was used in the simulations.

Using relationships established by Grilli and Watts (1999, 2001), Grilli et al (2002), Watts (1998 and 2000), and Watts et al (2003), an SMF was considered to be a wave maker whose shape and motion needed to be prescribed. The SMF was idealized as a mound (block) with elliptical cross-section translating along a straight incline at an angle θ to the horizontal. A maximum thickness T was defined in the middle of the mound, a total length b along the down-slope axis, a total width w along the cross-slope axis, and an initial vertical submergence d at the middle of the landslide. An elliptical platform, b by w, was also assumed for the SMF. The sliding mass was modeled as a rigid body moving along a straight incline with center of mass motion $s(t)$ parallel to the incline, and subject to external forces from added mass, gravity, and dissipation. COMCOT incorporates these relationships through the landslide tsunami source control files built into the system (Wang, 2009).

Assumptions were required for the volume and run-out distance of discharged SMF material. Volumetric estimations were based on contour interpolation of gravity data collected by Machesky (1965) - see Figure 8. The maximum volume of discharged material estimated from this reconstruction was 30 km^3. The maximum run-out distance of discharged material was estimated through 3D-exaggeration of bathymetry data in the Vulcan 7.5 software. Hummocky- type relief with 100 m amplitudes between troughs and peaks was noted approximately 30 km south of the island; these were assumed to represent the run-out maximum of the Ta'u SMF. Figure 9 and Figure 10 illustrates these assumptions.

A slide angle θ of 25^0 was used. The ratio of drop height to run-out distance h_0/x_c generally decreases with landslide volume (Ward and Day, 2003), and ranges from 0.05 to 0.15 for the Ta'u Island-sized (4 – 24 km^3) landslide. This implies a vertical mass drop height of about 1 – 3 km, and a run-out distance of about 20 - 30 km. A conservative volume of 4 km^3 was used in this study. The coefficient of basal friction μ, for low friction slides is approximately equal to h_0/x_c (Ward and Day, 2003). It was assumed here that $\mu \sim h_0/x_c$, hence a mean μ value of 0.1 was used. The mechanism inducing this low basal friction was assumed to be attributed to intense rock fragmentation that occurs in the basal region of large landslides (Davies & McSaveney, 2009; Davies et al, 2010), and has been inferred to act also in submarine mass movements. The Ta'u event appears to be similar to the 1884 Ritter Island collapse in Papua New Guinea (Ward and Day, 2003). A similar terrestrial analogy would be the debris avalanche of Mount St Helens volcano in 1980, where block-slides accelerated to speeds of over 50 ms^{-1} within 26 s and 700 m of the start time and location (Glicken, 1996; Voight et al, 1983; Ward and Day, 2003).

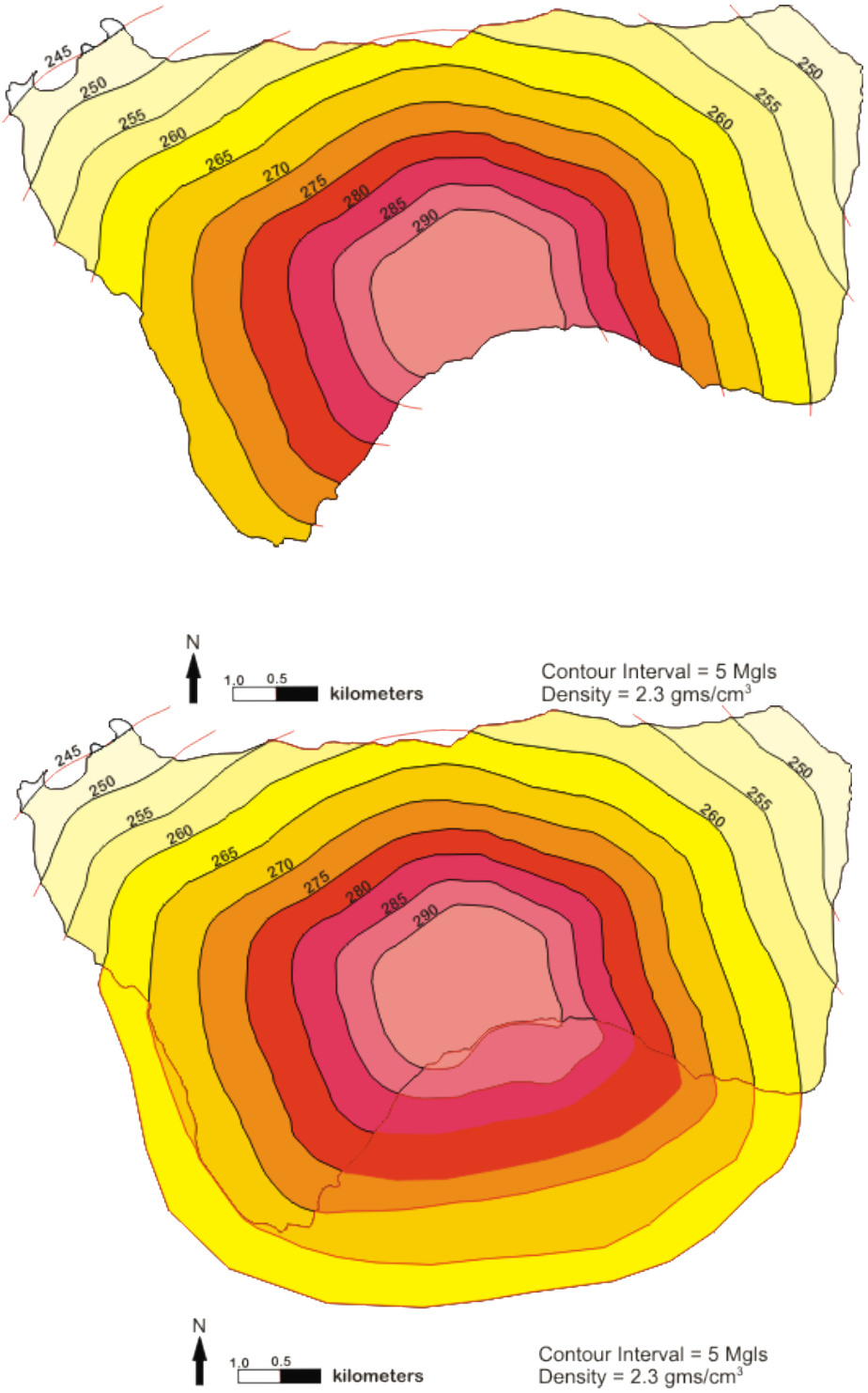

Figure 8: Gravity contour reconstruction using simple point interpolation, illustrating how the island may have looked in plan-view before (bottom image) and after (top image) to collapse.

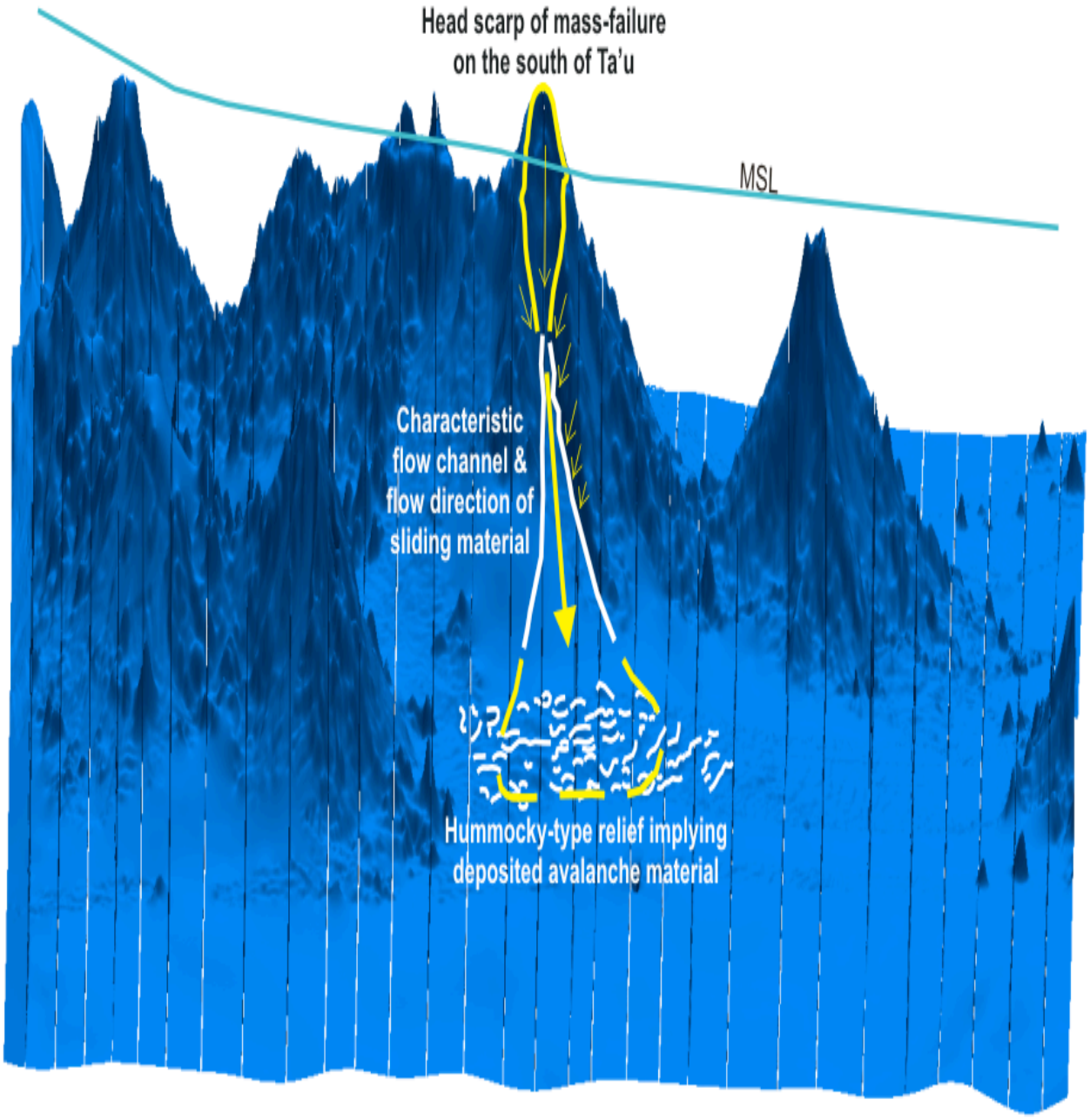

Figure 9: Exaggerated 3D-section view looking north at the southern flank of the Ta'u volcanic pile. Vertical lines shown across the N-S plane can be ignored. An offshore submarine flow channel and hummocky-type deposit are apparent south of the avalanche scarp.

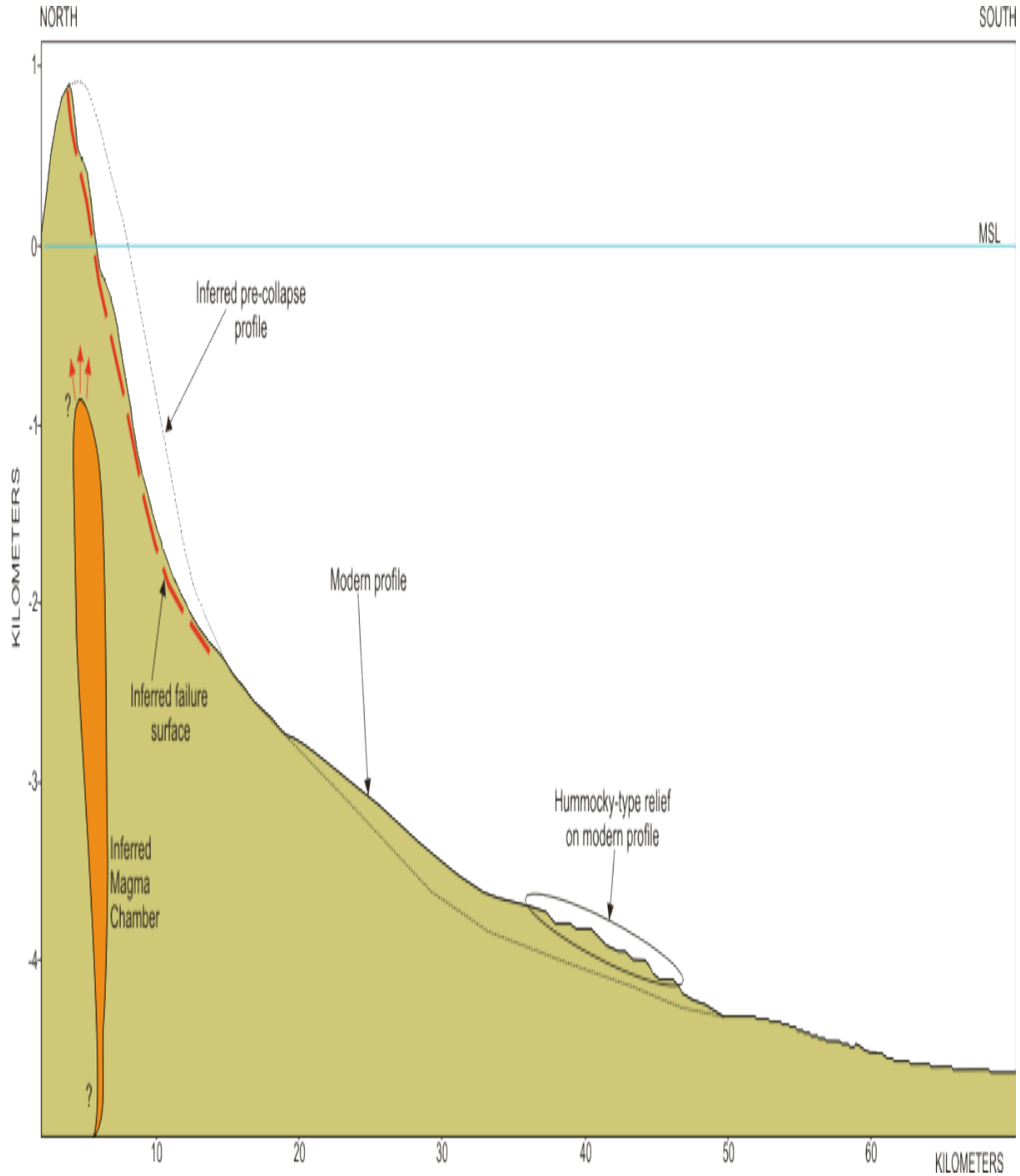

Figure 10: Cross-section of the south flank and offshore morphology of Ta'u. The inferred pre-collapse profile and failure surface are shown, as well as the inferred deposit denoted by the hummocky relief ~30km offshore.

3. RESULTS AND INTERPRETATIONS

3.1 Geomorphic and possible age interpretations

A geomorphic assessment of the south flank was undertaken to obtain a better understanding of the landscape features and processes on Ta'u, as well as their relative timing of formation.

The summit of Ta'u appears to be the northern caldera rim, which overlooks a series of down-faulted, approximately horizontal benches (Figures 2 and 3). Afuatai, the upper bench, is covered with thin-bedded horizontal flows of oceanite and olivine basalt, with a few small areas that are mantled by a 1 m bed of fine-grained tuff with laminate less than 1.3 cm thick. The lower bench, Ele'elesa, contains three large pit craters and a cinder cone, with a likely fault scarp marking the cliff-face down to the ocean. Lava flows exposed in the high fault-scarp bounding Afuatai bench to the summit of Lata mountain dip approximately 15^{o} away from the summit. Stice and McCoy (1968) suggested that the bench at Afuatai and the narrower benches to the southwest at Leavania, and to the southeast at Li'u, represent the former summit of the volcano, which has dropped approximately 450 m. They also suggested that the lower bench at Ele'elesa, the pit craters and the cinder cone, represent the original caldera of the volcano. The approximately horizontal bedding of flows comprising these benches relative to the average 15^{o} dip of flows in the southeast and west escarpments probably indicates a series of rotational slips along the fault-surface(s). Bathymetry and gravity data suggest that the caldera has no southern rim, as indicated by the steep drop of the seafloor to about 3000 m on the south side (Fenner et al, 2008).

Lava flows from the cinder cone eruption mapped separately in Figure 6 flow over the Ele'elesa scarp-face, indicating that it was deposited after collapse. This eruption may have been associated with the collapse, although any firm conclusions would be premature at this stage. If this were the case, it seems likely collapse was older than the 170 yr impression given by the map in Wilkes (1849). If the cinder cone eruption was historical and associated with the collapse, it would probably have been documented either through written or oral accounts. The absence of either of these leads to the belief that the eruption was pre-historic, probably $\geq$ 1 Ka; old enough to have disappeared from oral records (Linnekin et al, 1995). The young erosional gullies formed at the head of the north flank fault appear to be directly related to surface erosion. This flank also appears to be unbuttressed, meaning the likelihood of future collapse similar to the south flank could occur.

Erosional processes resulted in the formation of stream gullies and a 60 m sea cliff around most of the island, the northwestern portion being buried by the Faleasao formation. The sea-cliff here is thought to represent a wave-cut platform, formed during the sea level high-stand associated with the last interglacial maximum ~ 0.07 - 0.12 Ma. Bathymetry suggests that a submarine wave-cut platform encircles most of the island, and is assumed to have formed during the sea level low-stand associated with the last glacial maximum ~ 0.018 Ma. Large-scale catastrophic collapse or long-term slope failure (Stice and McCoy, 1968) resulted in the removal of the southern half of the original shield volcano - an estimated total volume of 4 – 30 km^3. This paper assumes the former. Both the sub aerial and submarine wave-cut platforms are absent on the south flank, leading to the belief that collapse occurred after their formation; i.e. < 0.018 Ma.

3.2 Modeling of the flank collapse and subsequent tsunami

The results discussed below assume the rapid collapse of a 4 km^3 mass along a slide angle θ of 25^0, with a run-out distance of 18.4 km. The length of the sliding mass = 3.2 km, width = 2.5 km, and thickness = 0.5 km. The 500 m drop of the present-day Afuatai bench from the Lata summit was assumed to be characteristic of the maximum thickness in the middle of the sliding block (Ward and Day, 2003). The specific density used was 2.2 (sliding mass density = 2300 kgm^{-3}: density of seawater = 1030 kgm^{-3}), and the coefficient of basal friction was 0.1. The simulated event run-time was 30 minutes (1800 s), and snapshots of ocean volume flux (flow per unit area) were recorded at 1-minute simulation intervals. Dispersion was ignored as shallow-water techniques were used. Figure 11 shows the simulated tsunami amplitudes and propagation at given times after landslide initiation. Figure 12 shows the main flux in the north-south and east-west directions.

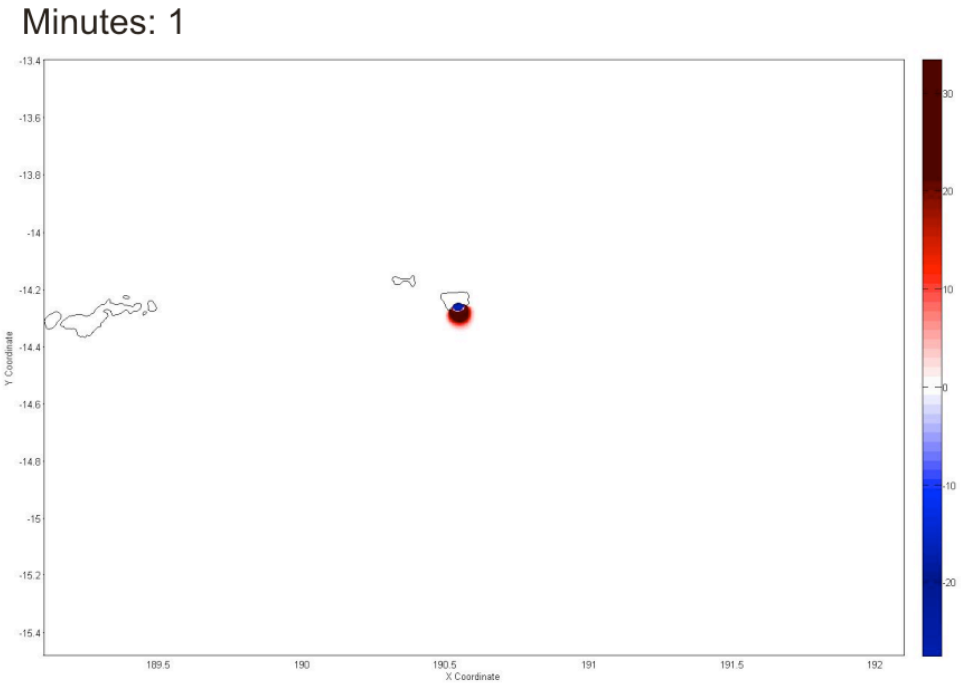

Minutes: 3

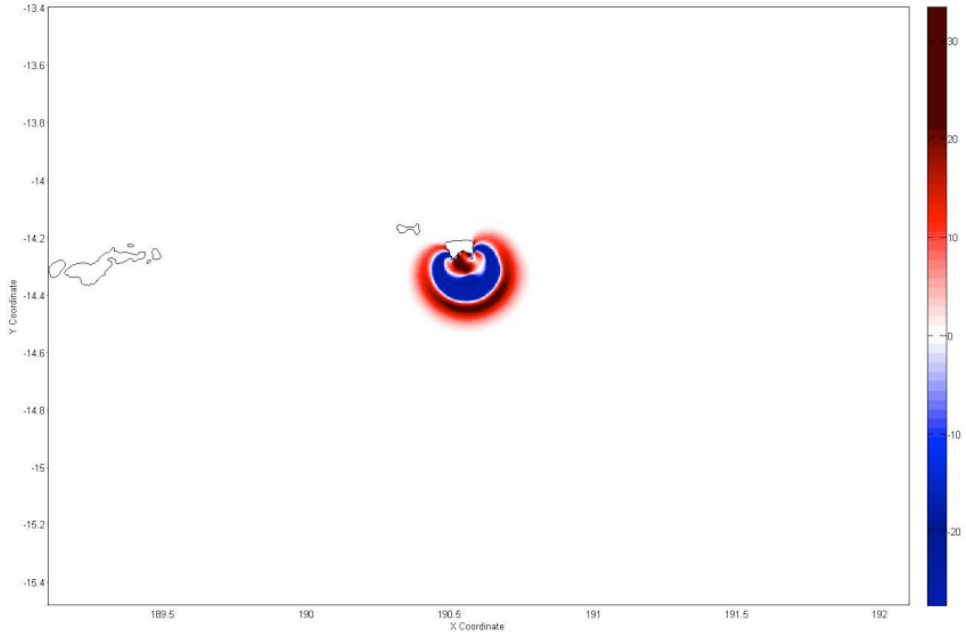

Minutes: 5

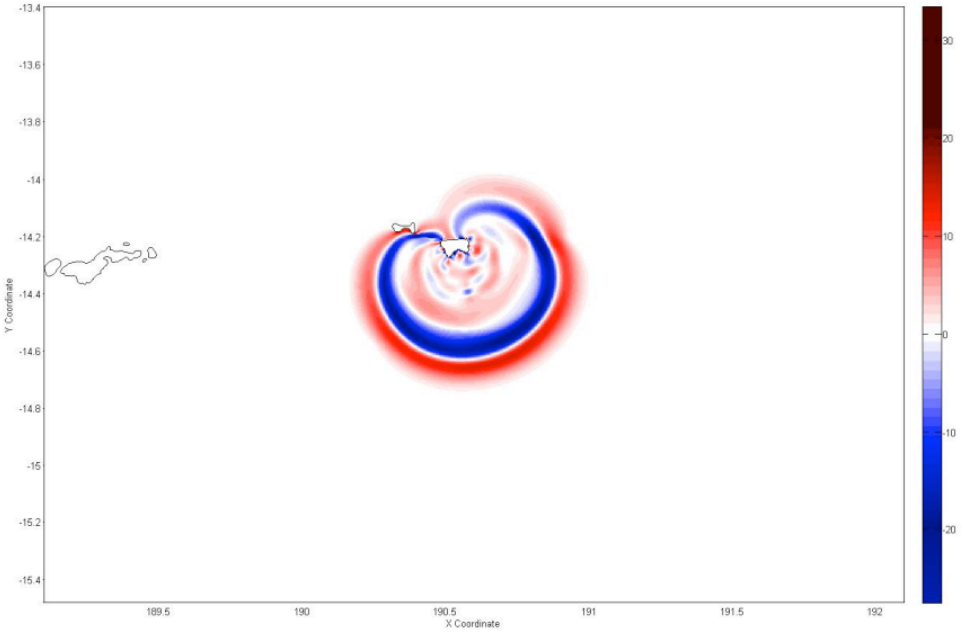

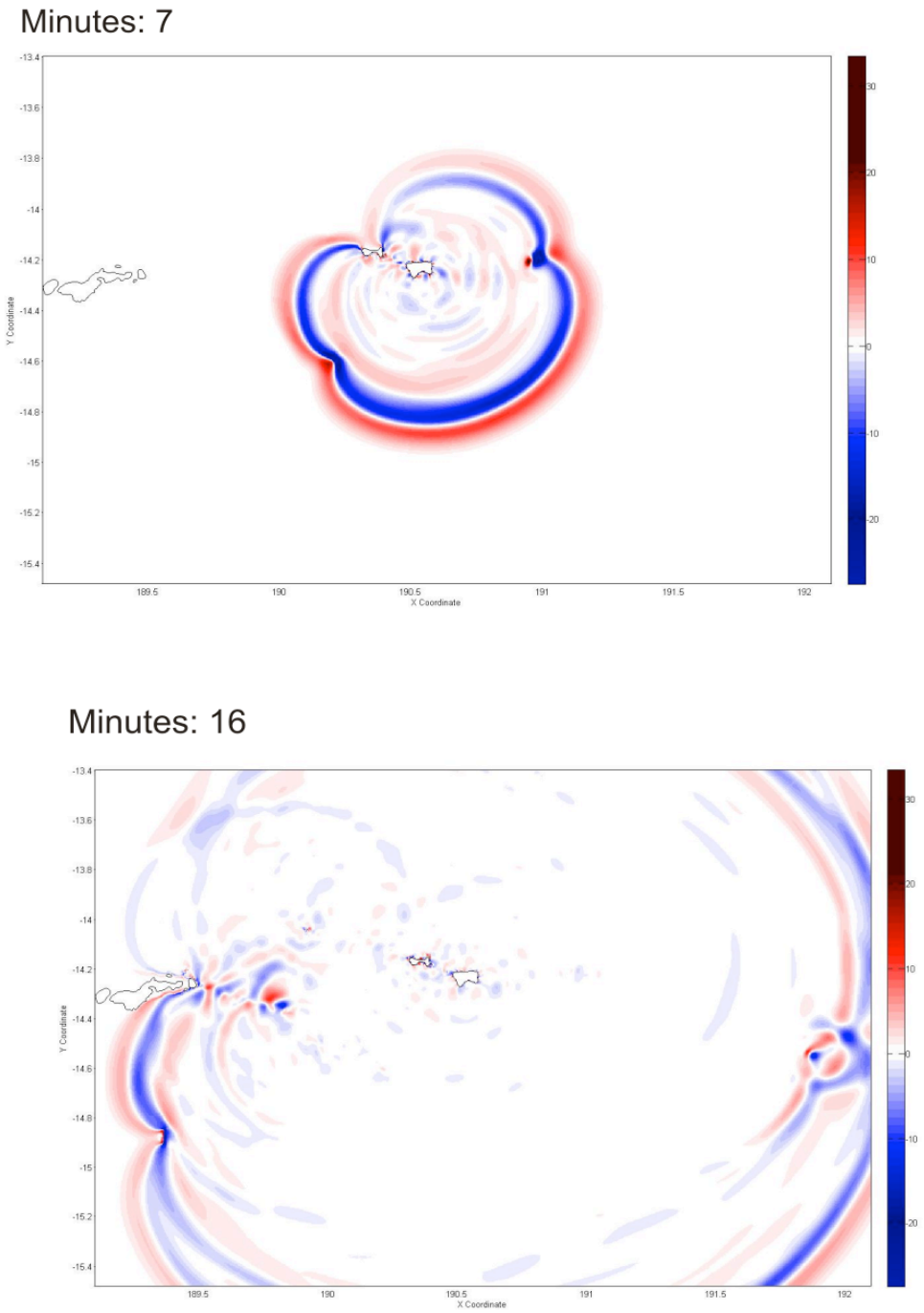

Figure 11: Simulated tsunami amplitude and flux ($m^3 \cdot m^{-2} \cdot s^{-1}$) predicted for the Ta'u collapse at 1, 3, 5, 7 and 16 minutes after initiation of the event.

The duration of the landslide determined in the idealized block-slide analysis was 7 minutes, with a peak slide velocity of 75.2 ms^{-1}. The average slide velocity was 43 ms^{-1}. Initial acceleration was 1.1 ms^{-2}, and deceleration of -0.1634 ms^{-2} began 1 minute after slide initiation; the mass slid for about 4.5 km before reaching the flat of the ocean floor at a depth of about 3 km. It slowed down for the remainder of the travel until it stopped approximately 18.4 km from source. The landslide generated a tsunami with amplitudes greater than 20 m propagating in all directions 5 minutes after slide initiation.

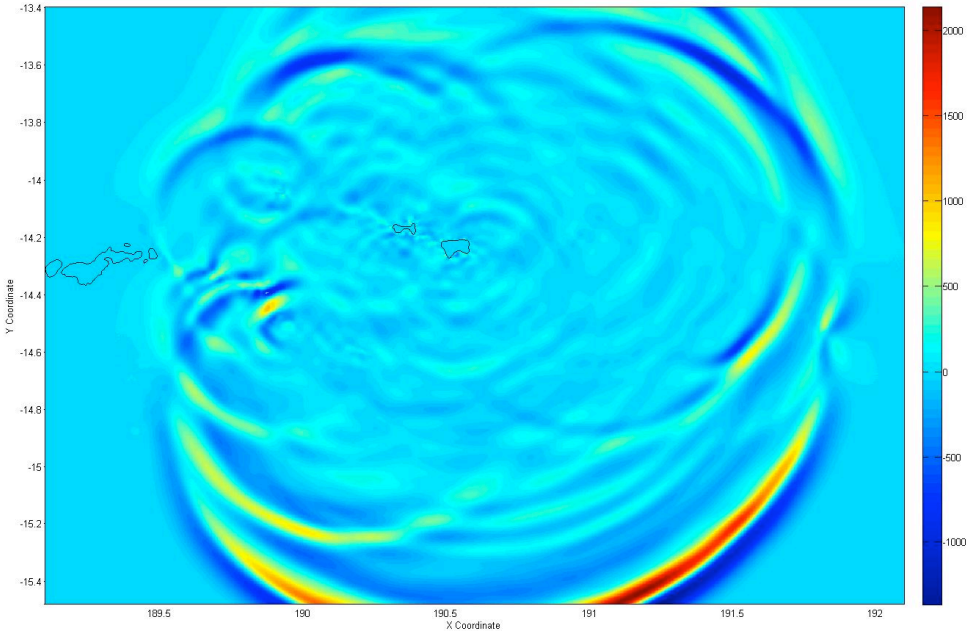

Figure 12: Direction of tsunami propagation in the X (north-south; top map) and Y (east-west; bottom map) axis. Main flux along the X-axis is southward, although sufficient wave diffraction around the island results in a northward propagating wave. Flux along the Y-axis is relatively proportional in both the east and west directions, respectively.

These effects are comparable with the Ritter Island collapse modelled by Ward and Day (2003). Their results showed a 4.6 km^3 landslide, which slid with an average velocity of 40 ms^{-1} (peak velocity near 70 ms^{-1}), and took about 5 minutes to run its course. The steep initial basal slope of 10 – 15^0 (peak of 25^0) in their model made for a short-lived acceleration phase. Having reached a decrease in basal slope, the slide spent much of the remainder of its movement travelling at a limiting speed. Friction coefficients used in their analysis ranged between 0.05 – 0.07. The simulation generated a tsunami with wave amplitudes of 20 m offshore of New Britain, compared to the actual 12 – 15 m elevation of inundation measured there. This difference was considered insignificant, and was

attributed to the short wave periods and loss of wave energy on the offshore reefs and in coastal trees as the wave approached and inundated the coast. The smaller debris avalanche of 0.05 – 0.09 km^3 which formed during the 26th December 1997 eruption of Soufrière Hills volcano on Montserrat, was immediately followed by an energetic pyroclastic density current that devastated 10 km^2 of the south-western volcano flank. The event generated local tsunamis which impacted Montserrat with maximum wave run-up heights > 10 m (Le Friant et al, 2006; Sparks et al, 2002; Voight et al, 2002).

The simulation results for the Ta'u block-slide seem consistent with the examples discussed above. The 0.1 coefficient of basal friction used was consistent with the h_0/x_0 ratio determined for the slide. This would have been sufficient to slow the sliding mass down to rest at about 18 km from its source. The rapid acceleration to a peak slide velocity of 75.2 ms^{-1} before slowing down was likely attributed to the steep initial basal slope of 20 - 25^0. Tsunami waves with amplitudes > 20 m were generated offshore. The main direction of tsunami propagation was southward. Wave diffraction around the island resulted in northward propagating waves.

The study showed that rapid flank collapse resulting in the present-day morphology of the south flank would have generated a tsunami propagating in all directions. Offshore wave amplitudes > 20 m would have reached the villages of Ta'u and Faleasao in the northwest, and Fitiuta in the northeast between 3 – 4 minutes after landslide initiation. Similar offshore waves would have reached the south coast of Ofu and Olosega islands about 5 minutes after initiation. Wave amplitudes between 10 – 15 m would have occurred offshore of Tutuila Island 104 km west of Ta'u at about 17 minutes after initiation. 10 – 15 m waves also propagated outside of the simulated numerical domain, possibly indicating that populated islands adjacent to, but outside, of the domain may have also experienced similar offshore tsunami amplitudes.

The island of Upolu, about 200 km west of Ta'u, may have experienced offshore wave amplitudes > 5 m in some areas, with smaller amplitudes experienced offshore of southeast areas on Savai'i, 100 km further west. Swains atoll about 380 km north-northwest may have experienced similar waves. Other places such as the high raised limestone island Niue 500 km south, the low-lying Pukapuka atoll in the northern Cook Islands > 500 km northeast, the Tokelau atolls > 500 km north, and Tafahi and Niuatoputapu islands in Tonga 480 km southwest, perhaps experienced waves < 2 m.

The likely elevation of inundation experienced at the northwest villages on Ta'u, and on Ofu and Olosega islands were probably several metres lower than the modeled offshore waves > 20 m. The village of Ta'u would most likely have experienced the greatest elevation of inundation (perhaps > 10 m), being the closest to the source and located < 10 m above mean sea level. The tidal range in the area is approximately 0.85 m (Izuka, 2005), meaning inundation would have occurred regardless of the time of the day. The fringing reef bounding the narrow lagoon about 100 m between the reef crest and the coastline would have induced short-period waves and loss of energy as the wave approached the coast. Limited coastal vegetation on the calcareous sedimentary unit < 10 m above mean sea level, would have meant probable inundation to the western base of the Tunoa shield between 100 – 400 m inland. Similar inundation impacts may have been experienced at Faleasao, and on Ofu and Olosega. The fringing reef surrounding Ofu and Olosega is greater than 200 m from crest to shoreline in most places, although > 95% of inhabited areas are situated < 10 m above mean sea level. The proximity of Fitiuta village in the northeast of Ta'u, > 25 m above mean sea level, would have meant that no inundation impacts were experienced at this site.

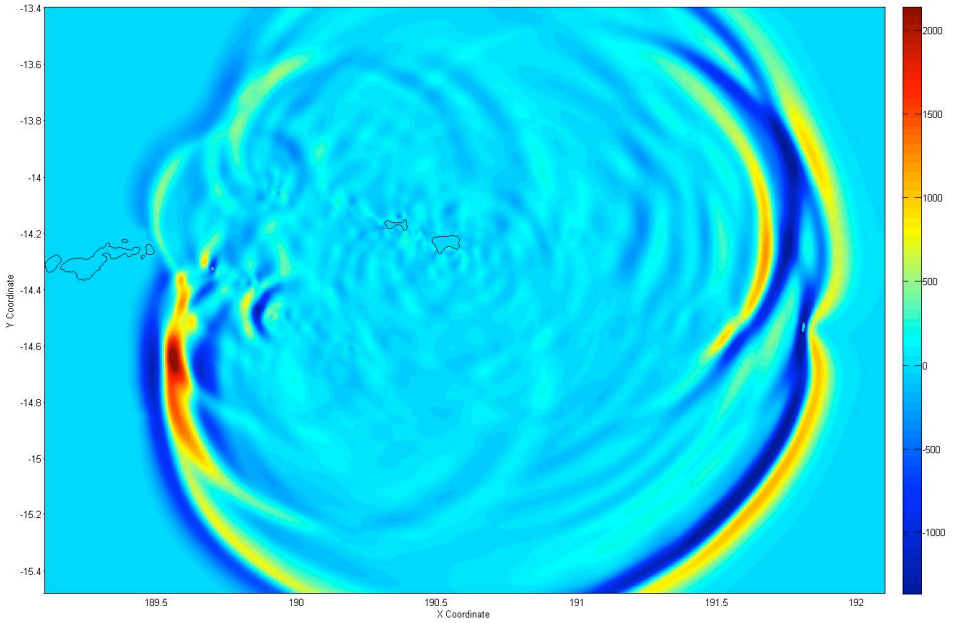

Figure 12: Direction of tsunami propagation in the X (north-south; top map) and Y (east-west; bottom map) axis. Main flux along the X-axis is southward, although sufficient wave diffraction around the island results in a northward propagating wave. Flux along the Y-axis is relatively proportional in both the east and west directions, respectively.

4. CONCLUSIONS

The modeled landslide-tsunami results demonstrate that if a historical collapse event occurred within the last 167 years resulting in the present day south flank morphology, the impacts could not have gone unnoticed by inhabitants of Ta'u and Faleasao villages on Ta'u Island, and inhabitants of Ofu, Olosega and Tutuila islands, respectively. It is likely that inhabitants on eastern and some southern areas of Upolu and Savai'i islands would have also noticed the impacts. There is no evidence of this in recorded history. This suggests that the depiction of Ta'u in Turner (1889), which was based on the original survey charts of Wilkes (1849), may have been incorrect, and the catastrophic collapse of the south flank and subsequent tsunami were much older.

The only alternative is that there were a series of smaller collapses requiring lower friction coefficients, and over a longer period of time. Smaller tsunami, which may have formed from these collapses, may not have had sufficient energy to diffract around the island and inundate exposed villages. However it seems unlikely that multiple collapses could have occurred in the last 170 years, without some record in the oral history.

ACKNOWLEDGEMENTS

We thank Dr. Gegar Prasetya and Dr. Xiaoming Wang of GNS Science NZ for their help regarding the use of the COMCOT numerical model. We acknowledge and thank NZAID and the Mason Trust, University of Canterbury for funding this research.

REFERENCES

Davies, T.R.H. and McSaveney, M.J., (2009). The role of rock fragmentation in the motion of large landslides. Engineering Geology. 109 (1-2): 67-79

Davies, T.R.H., McSaveney, M.J. and Kelfoun, K. (2010). Runout of the Socompa volcanic debris avalanche, Chile: a mechanical explanation for low basal shear resistance. Bulletin of Volcanology **72**:933–944 DOI 10.1007/s00445-010-0372-9

Fenner, D., Speicher, M., Gulick, S., (2008). The State of Coral Reef Ecosystems of American Samoa. In: Waddell, J.E. and A.M. Clarke (eds) 2008. The State of Coral Reef Ecosystems of the United States and Pacific Freely Associated States: 2008. NOAA Technical Memorandum NOS NCCOS 73. NOAA/NCCOS Center for Coastal Monitoring and Assessment's Biogeography team. Silver Spring, MD. 569 pp.

Glicken, H., (1996). Rockslide-Debris Avalanche of May 18, 1980, Mount St. Helens Volcano, Washington. Open-file Report 96-677. Cascades Volcano Observatory, Vancouver, WA 98661.

Grilli, S.T. and Watts, P., (1999). Modelling of waves generated by a moving submerged body: Applications to underwater landslides. Eng. Analysis with Boundary Elements. 23(8): 645-656.

Grilli, S.T. and Watts, P., (2001). Modelling of tsunami generated by an underwater landslide in a 3-D numerical wave tank. Proc. of the 11th Offshore and Polar Eng. Conf., ISOPE01, Stavanger, Norway. 3: 132-139.

Grilli, S.T., Vogelmann, S., Watts, P., (2002). Development of 3-D numerical wave tank for modeling tsunami generation for underwater landslides. Eng. Analysis with Boundary Elements 26(4): 301-313.

Hill, P.J. and Tiffin, D.L., (1993). Geology, sediment patterns and widespread deformation on the sea floor off Western Samoa revealed by wide-swath imagery. Geo-Marine Letters 13: 116-125.

Izuka, S.K., 2005, Reconnaissance of the Hydrogeology of Ta'u, American Samoa: U.S. Geological Survey Scientific Investigations Report 2004-5240, 20 p.

Keating, B.H., Helesley, C.E., Karogodina, I., (2000). Sonar studies of submarine mass wasting and volcanic structures off Savaii Island, Samoa. Pure and Appl. Geophys. 157: 1285-1313.

Keating, B.H., McGuire, W.J., (2000). Island Edifice Failures and Associated Tsunami Hazards. Pure and Appl. Geophys. 157: 899-955.

Le Friant, A., Boudon, G., Komorowski, J.-C., Heinrich, P., Semet, M.P., (2006). Potential Flank-Collapse of Soufrière Volcano, Guadeloupe, Lesser Antilles? Numerical Simulation and Hazards. Natural Hazards 39: 381-393.

Linnekin, J., Hunt, T., Lang, L., McCormick, T., (1995). Ethnographic Assessment and Overview: The National Park of American Samoa. Department of Anthropology, University of Hawaii.

Macdonald, G.A. and Abbott, A., (1970). Volcanoes in the Sea. University of Hawaii Press Honolulu, pp 137-147.

Machesky, L.F., (1965). Gravity Relations in American Samoa and the Society Islands. Pac. Sci. 19(3): 367-373.

Natland, J.H., (1980). The progression of volcanism in the Samoan linear volcanic chain. American Journal of Science 280-A: 709-735.

Natland, J.H. and Turner, D.L., (1985). Age progression and petrological development of Samoan shield volcanoes: Evidence from K-Ar ages, lava compositions and mineral studies. In: Brocker, T.M., (ed). Geological investigations of the northern Melanesian borderland: Houston, Texas, Council for Energy and Mineral Resources. Circum-Pacific Council for Energy and Mineral Resources Earth Science Series 3: 139-172.

Nunn, P.D., (1994). Oceanic Islands. Blackwell, Oxford.

Nunn, P.D., (1998). Pacific Island Landscapes: Landscape and Geological Development of Southwest Pacific Islands, especially Fiji, Samoa and Tonga. Institute of Pacific Studies, The University of the South Pacific, Fiji.

Sparks, R.S.J., Barclay, J., Calder, E.S., Herd, R.A., Komorowski, J-C., Luckett, R., Norton, G.E., Ritchie, L.J., Voight, B., Woods, A.W., (2002). Generation of a debris avalache and violent pyroclastic density current on 26 December (Boxing Day) 1997 Soufrière Hills Volcano, Montserrat. In: Druitt, T.H. & Kokelaar, B.P. (eds). The Eruption of the Soufrière Hills Volcano, Montserrat, from 1995 to 1999. Geological Society, London, Memoirs, 21: 409-434.

Stice, G.D., McCoy, F.W., (1968). The geology of the Manu'a Islands, Samoa. Pacific Sci. 22: 427-457.

Turner, G.A., (1889). Samoa. Scottish Geographical Magazine 5: 235 - 256.

U.S. Census Bureau, (2000). Census 2000 Data for American Samoa. Online at http://www.census.gov/census2000/americansamoa.html

Voight, B., Komorowski, J-C., Norton, G.E., Belousov, A.B., Belousova, M., Boudon, G., Francis, P.W., Franz, W., Heinrich, P., Sparks, R.S.J., Young, S.R., (2002). The 26 December (Boxing Day) 1997 sector collapse and debris avalanche at Soufrière Hills Volcano, Montserrat. In: Druitt, T.H., Kokelaar, B.P. (eds) 2002. The Eruption of Soufrière Hills Volcano, Montserrat, from 1995 to 1999. Geological Society, London, Memoirs, 21: 363-407.

Voight, B., Janda, R.J., Glicken, H., Douglass, P.M., (1983). Nature and mechanics of the Mount St. Helens rockslide-avalanche of 18 May 1980. Geotechnique 33: 243-273.

Wang, X., (February 2009). User Manual for COMCOT Version 1.7. Geological and Nuclear Sciences NZ, Wellington.

Ward, S.N., Day, S., (2003). Ritter Island Volcano - lateral collapse and the tsunami of 1888. Geophys. J. Int. 154: 891-902.

Watts, P., (1998). Wavemaker curves for tsunamis generated by underwater landslides. J. Wtrwy. Port, Coast, and Oc. Eng., ASCE 124(3): 127-137.

Watts, P., (2000). Tsunami features of solid block underwater landslides. J. Wtrwy. Port, Coast, and Oc. Eng., ASCE 126(3): 144-152.

Watts, P., Grilli, S.T., Kirby, J.T., Fryer, G.J., Tappin, D.R., (2003). Landslide tsunami case studies using Boussinesq model and a fully nonlinear tsunami generation model. Nat. Haz. Earth Sys. Sci. 3: 391-402.

Wilkes, C., (1849). Narrative of the United States Exploring Expedition during the years 1838, 1839, 1840, 1841, 1842, In five volumes with thirteen maps. Vol.1. U.S.N. Philadelphia.